Delft University of Technology

Bachelor Final Project Applied Physics
TN2983

An emergency cooling system for SLIMR, the supercritical-water Small, Modular Reactor

Author:
Sebastiaan J. Ettema (4311477)

Supervisor:
Dr. Ir. M. Rohde
Department of RPNM

Thesis committee:
Dr. Ir. M. Rohde
Dr. Ir. D. Lathouwers

February 19, 2018

Abstract

Since the Fukushima incident in 2011, there is an increasing interest in a new type of reactor: the Small Modular Reactor (SMR). SMRs have the ability to remove the decay heat passively to the environment increasing safety, and their modularity increase employment variety and offers a good investment opportunity. Rohde [4] proposed a design of a type of SMR: the SLIMR (a Small-scale, Large efficiency, Inherently safe, Modular Reactor). Veling [3] and Krijger [5] adopted this design and made improvements on safety and efficiency.

Veling and Krijger both proposed in their research that it might be interesting to research the feasibility of a second containment around the reactor where an air pressure is kept with a pump while operating normally with the goal to decrease heat loss during normal operation. In situation of SCRAM, the pump will shut off and a valve will open. Due to pressure difference this insulation tank fills with water and passively loses the decay heat. This research gives a first insight in the filling time of such an insulation tank and will do an approximation of the temperature increase inside the reactor before the cooling process starts.

To calculate the filling time, the mechanical energy balance is used. The mechanical energy balance is calculated in discrete time and the result is approximated using an explicit as well as an implicit method. Due to stability problems using the explicit solution there is chosen to work with the implicit solution for determining the role of the geometrical factors. This research proposes a geometry with which the insulation tank is filled in $8.14[s]$.

There are four geometrical factors affecting the system: the annulus diameter, the entrance cross-sectional area at the bottom of the tank, the depth of the tank in the pool and the inlet friction factor. The annulus diameter and entrance cross-sectional area have the largest effect on the time, therefore they are optimized. To calculate the temperature increase constant pressure is assumed and the start of the cooling process is determined at half the filling time. With the proposed geometry the temperature increases approximately with $0.35[K]$.

The increase in temperature is considered reasonable and therefore follow-up research with the heat transfer is recommended. This research should investigate the safety of the reactor under the new circumstances and consider as well whether the insulation containment leads to operational benefits.

Contents

Chapter 1

Introduction

In the year 2011, the Fukushima disaster occurred[1]. The cause was an energy accident initiated by a tsunami with subsequent seaquake. Immediately after the earthquake, the active reactors automatically shut down their sustained fission reactions. However, the tsunami disabled the emergency generators that would have provided power to control and operate the pumps necessary to cool the reactors. The insufficient cooling led to three nuclear meltdowns, hydrogen-air explosions, and the release of radioactive material.

Before this disaster, the support of nuclear energy was growing in the world [2]. This accident reduced the support. But the energy consumption in the world is growing fast and it is expected to do so in the near future. With the concern of climate change due to the emission of CO_2, and the fact that renewable energy will be insufficient to meet the demand in the world fast, nuclear energy is expected to still be an important contributor to a more sustainable energy production.

To add strength to this idea, the Generation IV International Forum was founded. With the Fukushima accident in mind, the major improvements that would be made are improvements in the safety of nuclear power plants. This resulted in six innovative reactor types, all developed towards the so-called Small Modular Reactors (SMRs). The SMR has a relatively low power density in relation to the size of the reactor. This creates the possibility to remove decay heat completely passively (i.e. without the use of external power sources) in the event of a station blackout, increasing the safety of nuclear reactors [3].

The Small-scale Large efficiency, Inherent safe Modular Reactor (SLIMR) as proposed by Rohde [4] also has the ability to cool itself passively. One of the reasons it can do so, is because the surface of the reactor to his surroundings is relatively large. This increases the safety when there is a breakdown in the reactor, but also increases heat loss during normal operation. Therefore, Krijger [5] recommended that an insulation cylinder could be examined that could fill itself passively with water in the situation of a breakdown.

This research will give a first insight in the geometry of such an insulation tank. There will be determined which factors are important in slowing down or accelerating the process, and how these factors can be used in their benefit.

1.1 The SLIMR

1.1.1 Small Modular Reactors

Before continuing expiring on the SLIMR, first the advantages and challenges of the new generation SMRs are being discussed. This advantages and challenges will be compared with the existing use of the Large Reactors (LRs).

The most important advantage of the SMRs is that they are possible to remove their decay heat passively during emergency scenarios. Secondly, because of their smaller scale, SMRs can meet local power demands on much smaller sites than LRs [5]. Where LRs can exceed the local power demand and therefore bring economical constraints, SMRs can meet the local power demand flexibly by adding more SMRs. Thirdly the modularity of SMRs makes them suitable for more operations than only producing electricity. SMRs can also be used for producing heat and the desalination of water [6]. LRs can be used for these purposes as well, but have a higher chance of exceeding the power demands for this processes.

There are also some economical benefits to the SMRs. Because they can be fully produced off site and transported to the location, no work on site has to be done. Also, when manufacturing is done on a single SMR or an accident on one SMR occurs, the other SMRs are not affected by this and can continue producing energy. The economical advantages of LRs were in the economies of scale. As the capacity of a reactor increases, the average investment and operating cost per unit of energy decreased. Though, SMRs have a advantage in economies of mass. Because SMRs have the ability to be produced in a factory as a whole, increasing and standardizing their production can lead to a large decrease in cost.

If there were only advantages on the SMRs, why are they not used on larger scale at the moment then? Firstly, it is important to mention that calculations on natural circulation require sophisticated computer simulations, which were not available for a long time (20 or 30 years ago) [5]. Secondly, though modularity seems like a big advantage for SMRs, plants with smaller capacity (under $1[GW]$) seem to have less economical benefit to this. The reason for this is that fixed costs and investments are spread over a lower power capacity which makes smaller nuclear projects less interesting. Finally, nuclear projects often have long license processes and much regulatory issues. Therefore, new techniques and projects that are not used anywhere else can experience many hurdles to get their licensing done [5].

1.1.2 The SLIMR design

In the last section is explained why transferring from LRs to SMRs could be beneficial. Now is devoted further on the design of the SLIMR. The SLIMR design is initially proposed by Rohde [4] of the department of RPNM at the Reactor Institute Delft with the goal to increase the safety as well as the efficiency of the SMRs. The SLIMR is a SMR design which is inherently safe. With inherently safe is meant that the reactor is able to be cooled without the addition of any active system (f.e. pumps).

The SLIMR is a nuclear reactor driven on naturally circulated flow under high pressure ($25[MPa]$). In latest research done by Krijger [5] the SLIMR produces a power of $350[MWth]$. The SLIMR has the highest efficiency when the water surpasses a pseudo-critical temperature of $375[°C]$, because then the density of water decreases significantly. In Krijgers report the core outlet temperature reached $396[°C]$ and therefore benefits from the pseudo-critical state of the water.

The original proposed geometry by Veling [3] of the SLIMR is shown in figure (1.1). The water passes through the core where the coolant is heated. Because the density decrease the fluid streams upward through the riser and through the heat exchanger. There the coolant is cooled down by flowing through the heat exchanger, the density increases and flows down through the downcomer reaching the core again. Krijger changed the geometry of the core, extending the path of the water through the core and therefore making possible that the core outlet temperature exceeded the pseudo-critical temperature.

The water inside the reactor is held on a $25[MPa]$ pressure by the reactor pressure vessel (RPV) which has a wall thickness of $0.37[m]$. The reactor is submerged in a large pool. Because of the large surface of the RPV in comparison with the heat produced, the reactor is able to transfer its decay heat during accident scenarios through passive heat transfer mechanisms.

1.2 Outline and objectives of this thesis

The ability of the reactor to cool itself passively after a station blackout is an important feature of the reactor. But during normal operation the reactor also has significant heat losses to the pool because of its large surface adjacent to the pool. Therefore Krijger [5] proposed to design a second cylinder around the reactor, where during nominal operation a pump maintains air under pressure inside this cylinder. In a situation of SCRAM the pump shuts off, air flows out through a valve at the top lowering pressure, and water will flow inside this annulus through an opening at the bottom of the tank.

Doing this, heat losses during normal operation are expected to have a significant decrease, while cooling the reactor passively in scenarios of SCRAM might still be possible. This thesis will give a first insight in the geometry of such an insulation tank and what the possible filling speed of this tank can be. Also, there will be determined which are the factors that influence the filling speed and how strongly they affect the speed. In addition, an approximation of the temperature increase during this process is done to determine if follow-up research might be relevant.

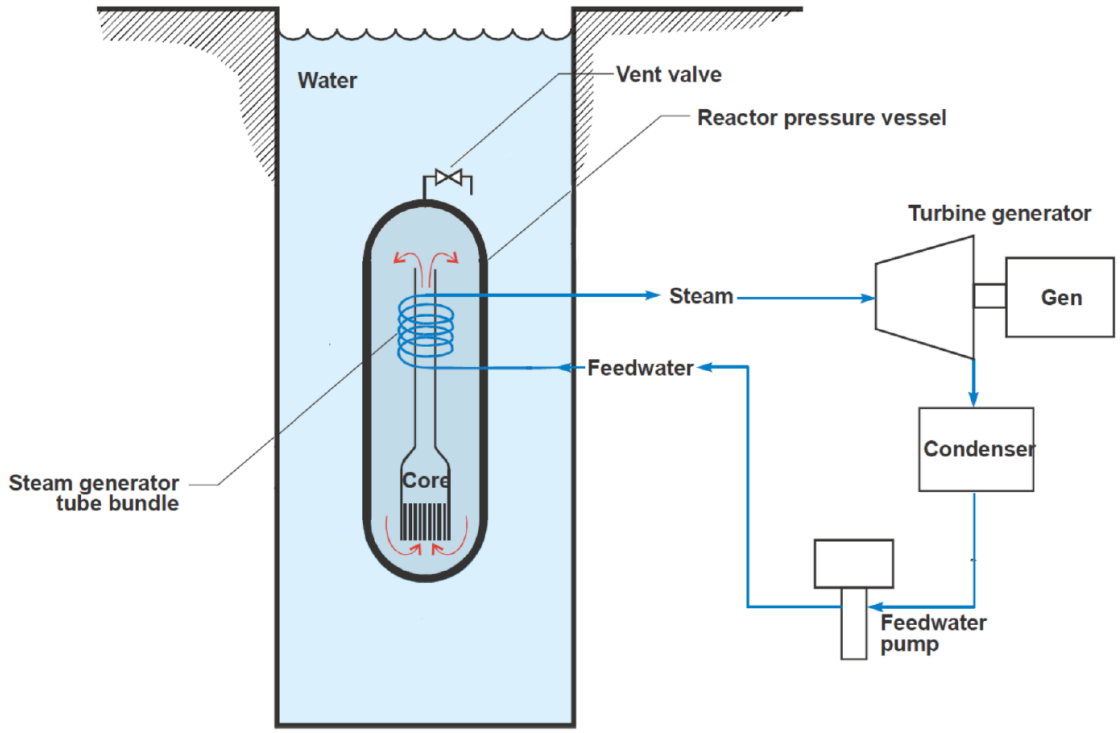

Figure 1.1: The design of the SLIMR as proposed by Veling [3]

The main research questions are determined as follows:

- How fast can the insulation tank fill itself with water in a situation of SCRAM?
- Which geometrical factors play a role determining the filling speed and how do they influence the system?
- Is the insulation tank a realistic option to solve the heat loss problems during normal operation and is there a possibility that the reactor still inherently safe?

The goal of the first question is to give an insight in the filling time and as handle during heat transfer calculations. The second question is important because when follow-up study treats the heat transfer these dimensional factors are also investigated and changed for optimizing the heat transfer. Therefore, this research should not only impose a geometry of the tank. This research must be flexible to geometrical changes that could be beneficial for the heat transfer. The third question is to determine whether follow-up study is relevant at all. If it is practically impossible to fill the tank fast enough to start the cooling process in time, follow-up study will not even be necessary.

In chapter (2), the theory behind this project will be explained. The next chapter, chapter (3), there will be elaborated on the numerical models used in this project and why they are used. In chapter (4), the results of this project will be given. And finally, in chapter (5), the conclusion and recommendations for follow-up study will be given.

Chapter 2

Theory

This chapter consist the theory used during this research. First, in section (2.1), the mechanical energy balance is given and further explained. In section (2.2) the mechanical energy balance for the system used in this research is given. In section (2.3) the mathematics used in this research are explained. Section (2.4) is devoted to the calculations with the decay heat and finally section (2.5) shows how the resulting increase in temperature due to the decay heat is calculated.

2.1 The mechanical energy balance

The mechanical energy balance consist of the change of energy inside the system, the flow of mass and takes into account the pressures, heights, velocities and friction factors inside the system. A schematic drawing of the mechanical energy balance over the insulation tank is given in figure (2.1). The standard mechanical energy balance is given by [7]:

$$\frac{dE_{tot}}{dt} = \phi_{m,in}(\frac{1}{2}v_1^2 + gh_1) - \phi_{m,out}(\frac{1}{2}v_2^2 + gh_2) + \phi_{work} + \phi_{pump} - \phi_{m,in}e_{diss} \tag{2.1}$$

With $\frac{dE_{tot}}{dt}$ as the change of energy $[\frac{kgm^2}{s^2}]$ differentiated over time. $\phi_{m,in}$ as the mass flow going inside the tank $[\frac{kg}{s}]$, this is the equal to the water flowing inside through point 1 in figure (2.1). $\phi_{m,out}$ is the mass flowing out of the control volume, which is none because the control volume is equal to the water surface (point 2) during the project. As a result, $\phi_{m,out}$ is zero. v_1 is the velocity $[\frac{m}{s}]$ of water far from the entrance which is zero. g is the gravity constant which equals $9.81[\frac{m}{s^2}]$. $h_1[m]$ is the height at the bottom of the insulation tank, which is determined as being zero. ϕ_{work} $[\frac{kgm^2}{s^2}]$ is the work done by the pressures on the total system. In this system these are the pressures at the entrance and at the surface of the water inside the annulus. In section (2.1.2), this term will be explained. ϕ_{pump} $[\frac{kgm^2}{s^2}]$ is the power supply through active systems, for example a pump. For the safety of the reactor it is important that it does not depend on active systems when a breakdown occurs. Therefore, ϕ_{pump} is zero during the project. At last, e_{diss} is the dissipated energy due to friction in $[\frac{m^2}{s^2}]$. So far formula (2.1) can be rewritten as follows.

$$\frac{dE_{tot}}{dt} = \phi_{work} - \phi_{m,in}e_{diss} \tag{2.2}$$

The mechanical energy balance for this system is thus only dependent on the change of energy in the system, with as driving force the pressure differences and some loss of energy due to the friction in the system. To understand formula (2.2) better, this formula will be explained further in the following sections.

2.1.1 Energy differentiated over time

This project is taking place in an unsteady state. This means the total mechanical energy inside the system changes over time. The total mechanical energy has a kinetic energy and a potential

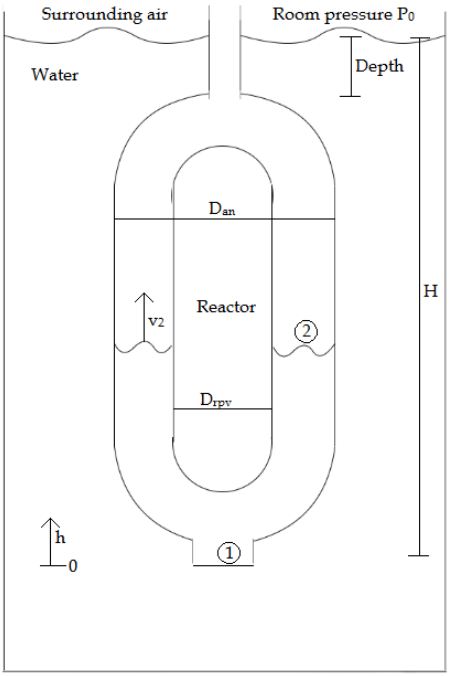

Figure 2.1: Simple schematic drawing of the reactor with insulation tank inside a pool showing variables and the points determining the control volume.

energy part.

$$\frac{dE_{tot}}{dt} = \frac{dE_{kin} + dE_{pot}}{dt} = \frac{dE_{kin}}{dt} + \frac{dE_{pot}}{dt} \tag{2.3}$$

In this formula E_{tot} is the total mechanical energy, E_{kin} is the kinetic energy and E_{pot} the potential energy in the system in $[J]$. In terms of other SI units this is $[\frac{kgm^2}{s^2}]$.

Kinetic energy

Kinetic energy is energy formed by the movement of mass. The interest lies in this research on determining the change in kinetic energy over time. Therefore the kinetic energy is differentiated over time.

$$\frac{dE_{kin}}{dt} = \frac{\rho_w A_{an}}{2} \frac{dh(t)v(t)^2}{dt} = \frac{\rho_w A_{an}}{2} (v(t)^2 \frac{dh(t)}{dt} + h(t) \frac{dv(t)^2}{dt}) \tag{2.4}$$

In this equation ρ_w is the density of water in $[\frac{kg}{m^3}]$ and $A_{an}[m^2]$ is the cross-sectional area of the annulus of the tank. The height at time t, $h(t)$ $[m]$, is dependent on $v(t)$ $[\frac{m}{s}]$. The relation between height and velocity is given in the next formula.

$$\frac{dh(t)}{dt} = v(t) \tag{2.5}$$

The relationship in formula (2.5) as well as the chain rule are used to rewrite formula (2.4).

$$\frac{dE_{kin}}{dt} = \frac{\rho_w A_{an}}{2} (v(t)^3 + h(t) \frac{dv(t)^2}{dt}) = \rho_w A_{an} (\frac{1}{2} v(t)^3 + h(t) v(t) \frac{dv(t)}{dt}) \tag{2.6}$$

Potential energy

The potential energy equation for the system described is written as follows.

$$E_{pot} = \int_0^{h(t)} \rho_w A_{an} g z dz = \rho_w A_{an} g (\frac{1}{2} h(t)^2) \tag{2.7}$$

In formula (2.3) the potential energy is differentiated over time and therefore it is rewritten as follows.

$$\frac{dE_{pot}}{dt} = \rho_w A_{an} g(\frac{1}{2}\frac{dh(t)^2}{dt}) = \rho_w A_{an} g(h(t)\frac{dh(t)}{dt}) = \rho_w g A_{an} h(t) v(t) \tag{2.8}$$

In the last step formula (2.5) is used again. Be aware that the potential energy increases. This might feel contradicting because the potential energy seems to be the driving force of the flow of water. That is in fact true, but because our mechanical energy balance is taken only inside the insulation tank, potential energy increases.

The total mechanical energy

By using formula (2.6) and (2.8) it is possible to determine the change in total mechanical energy in the system.

$$\frac{dE_{tot}}{dt} = \frac{dE_{kin}}{dt} + \frac{dE_{pot}}{dt} = \rho_w A_{an}(\frac{1}{2}v(t)^3 + h(t)v(t)\frac{dv(t)}{dt}) + \rho_w g A_{an} h(t) v(t) \tag{2.9}$$

This can be used in formula (2.2).

2.1.2 Work on the system due to pressures

At both top and bottom of the system there are pressures working. These pressures are different and both have a different source maintaining the pressure. There is a pressure at the bottom pushing the water into the insulation tank due to the height differences of the water. At the same time pressure inside the insulation tank is maintained by a pump. Before the flow of water starts, the pressures are in balance at the bottom entrance of the tank. As a result, the insulation tank is filled with air. When the pressure maintained by the pump falls away, the water begins to flow.

Pressure at the bottom of the tank

The driving force of the filling of the tank is the pressure at the bottom of the tank, which exists due to the height differences of the surfaces of the water in the insulation tank and at the top of the pool. The pressure at the bottom of the tank is equal to the air pressure with in addition the pressure due to the height difference. The total pressure at the bottom can be written as follows.

$$P_b = P_0 + \rho_w g H \tag{2.10}$$

Here, P_b is the total pressure at the bottom of the insulation tank in $[\frac{N}{m^2}]$, $P_0[\frac{N}{m^2}]$ the air pressure inside the room. $H[m]$ is the total height difference between the bottom of the insulation tank and the surface of the water inside the surrounding pool. To convert this pressure into work done over the system, the pressure has to be multiplied with the area on which it works, giving the force on the system due to this pressure. Then, this force is multiplied by the distance covered due to the force which gives us the work on the system. The work done at the bottom is determined as follows.

$$W_b(t) = A_{an} h(t)(P_0 + \rho_w g H) = \rho_w A_{an} h(t)(\frac{P_0}{\rho_w} + gH) \tag{2.11}$$

To determine $\phi_{work,b}$ the work done must be differentiated over time, which gives the following equation.

$$\phi_{work,b}(t) = \frac{dW_b(t)}{dt} = \rho_w A_{an}\frac{dh(t)}{dt}(\frac{P_0}{\rho_w} + gH) = \rho_w A_{an} v(t)(\frac{P_0}{\rho_w} + gH) = \phi_{m,in}(t)(\frac{P_0}{\rho_w} + gH) \tag{2.12}$$

The work on the system therefore is dependent on the mass flowing into the system. The equation for mass flow is given in formula (2.19). Normally, the pressure is therefore written as dependent on the mass flow at point 1 and point 2 inside the brackets in the mechanical energy balance (2.1). But in this project there is no outflow of mass because the control volume changes with the flow of the water. Despite, there is a pressure working on the surface of the water inside the insulation tank. Therefore, the pressures are determined as external work sources on the surface of the control volume.

Pressure at the water surface inside the insulation tank

At the surface of the water in the insulation tank, there is a pressure equal to P_b in formula (2.10) when the reactor is in normal operation. But, in situation of SCRAM, the pump maintaining this pressure shuts down and pressure is falling down back to the normal air pressure in the room (P_0). The pressure at the water surface is thereby given with the following formula.

$$P_s = P_0 + \rho_w g H * F(t) \tag{2.13}$$

Notice that this is almost the same equation as formula (2.10), the only difference is that the last term of the equation is multiplied by some function $F(t)$. This function determines the pressure fall of the air inside the insulation tank. In this project is assumed that the air pressure drops instantaneously down to zero. When t is zero, the pump shuts down and a valve at the top opens and pressure falls away. In reality, however, the pressure does not fall away instantaneous, but that assumption is made in this research. In following research it is possible to calculate the pressure change over time and thereby differ the value for $F(t)$. In this project the following relation is used.

$$\begin{aligned} F(t) &= 1 \text{ for } t \leq 0 \\ F(t) &= 0 \text{ for } t > 0 \end{aligned} \tag{2.14}$$

Similar to (2.1.2), the pressure at the surface can be rewritten as work done at the water surface.

$$W_s(t) = A_{an}(-h(t))(P_0 + \rho_w g H * F(t)) = -\rho_w A_{an} h(t)(\frac{P_0}{\rho_w} + gH * F(t)) \tag{2.15}$$

To determine the $\phi_{work,s}$, the function is differentiated over time. This is the same as is done in (2.1.2).

$$\begin{aligned} \phi_{work,s}(t) = \frac{dW_s(t)}{dt} = -\rho_w A_{an} \frac{dh(t)}{dt}(\frac{P_0}{\rho_w} + gH * F(t)) = \\ - \rho_w A_{an} v(t)(\frac{P_0}{\rho_w} + gH * F(t) = -\phi_{m,in}(t)(\frac{P_0}{\rho_w} + gH * F(t)) \end{aligned} \tag{2.16}$$

This project only works with time larger than zero, therefore the formula can be rewritten to the following.

$$\phi_{work,s}(t) = -\phi_{m,in}(t)(\frac{P_0}{\rho_w}) \tag{2.17}$$

Total work on the system due to pressures

If formula (2.10) and (2.16) are added up the total work due to pressure on the system is given.

$$\phi_{work}(t) = \phi_{work,b}(t) + \phi_{work,s}(t) = \phi_{m,in}(t) g H (1 - F(t)) = \phi_{m,in}(t) g H \tag{2.18}$$

The last term holds for time $t[s]$ larger than zero.

2.1.3 Mass flow and dissipated energy due to friction and appendages

In this section more information is given about the mass flow and dissipation energy used in formula (2.1). The mass flow is how much water flows in the tank over time. The friction is needed to calculate how much energy is lost on friction to the walls and entrance(s) of the tank.

Mass flow

The mass flow ϕ_m is dependent of the speed and surface of the annulus of the insulation tank, and is given by:

$$\phi_m = \phi_{m,in}(t) = \rho_w A_{an} v(t) \tag{2.19}$$

In this formula, A_{an} is again the surface of the annulus in $[m^2]$. Because the mass flow is dependent of $v(t)$, the mass flow too is dependent of time.

Reynolds number

The Reynolds number (Re) is a dimensionless number [$-$] used to calculate the ratio of inertial forces to viscous forces for given flow conditions. The Reynolds number describes whether there is laminar or turbulent flow using the flow conditions. The formula for the Reynolds number is as follows:

$$Re = \frac{\rho_w v(t) D_h}{\mu} \tag{2.20}$$

Here D_h is the hydraulic diameter of the annulus in $[m]$. The method to calculate the hydraulic diameter is given in formula (2.23). μ equals the dynamic viscosity of water in $[\frac{kg}{ms}]$.

The Darcy-Weisbach friction factor

The Darcy-Weisbach friction factor, $f[-]$, is a necessary factor for calculating the friction of the fluid inside the cylinder. The factor is given by some empirical correlations with the Reynolds number.

The approximation of the value of the Darcy-Weisbach friction factor differentiates between different ranges of the Reynolds number. In this project the Reynold number works between the range of approximately $10^5 < Re < 10^7$. Hence, the empirical formula of Haaland is used. This approximation is accurate for $Re > 3000$.

$$\frac{1}{\sqrt{f}} = -1.8 log_{10}(\frac{6.9}{Re}) \tag{2.21}$$

Because the Reynolds number consists of the speed $v(t)$ of the fluid, the Darcy-Weisbach friction factor is dependent on the velocity of the fluid inside the annulus. Formula (2.21) can be rewritten as:

$$f = (\frac{1}{-1.8 log_{10}(\frac{6.9}{Re})})^2 \tag{2.22}$$

The Darcy-Weisbach friction faction is a dimensionless number [$-$].

The hydraulic diameter

The hydraulic diameter D_h $[m]$ is a ratio between the surface of the cross section of the tank A_{an} and the moistened perimeter of the tank. This ratio is calculated to determine the degree of friction through the shape of the insulation tank. The formula for the hydraulic diameter and how it can be written is shown.

$$D_h = \frac{4A_{an}}{S} = 4\frac{\frac{1}{4}(D_{an}^2 - D_{rpv}^2)}{D_{an} + D_{rpv}} = D_{an} - D_{rpv} \tag{2.23}$$

Here, the moistened perimeter of the tank is S $[m]$. D_{an} is the diameter of the outer annulus in $[m]$ and D_{rpv} is the diameter of the reactor pressure vessel in $[m]$. During this project the hydraulic diameter is kept constant. Because of the hemispheric geometry of the insulation tank in reality this is not true.

Resistance coefficient K

Due to the appendages at the entrance of the system, resistance coefficient K_{tot} is introduced. This is a dimensionless [$-$] number, determined by the geometry of the entrance. To calculate the friction due to appendages, K_{tot} is multiplied by the velocity at the entrance squared. However, the velocity at the entrance is different from the velocity in the annulus. Therefore K_{tot} is corrected by dividing the velocity by the cross-sectional area of the entrance A_{en} and multiply by the cross-sectional area of the annulus A_{an}. As a result is the difference in velocity taken into account for the friction calculation. Therefore, the friction due to appendages in the system is given by the following equation.

$$e_{app} = K_{tot} \frac{A_{an}^2}{A_{en}^2} * \frac{1}{2} v(t)^2 \tag{2.24}$$

Here K_{tot} is the resistance coefficient determined by the geometry of the entrance of the insulation tank, where the cross-sections correct the velocity is the annulus $v(t)$ to the velocity of the entrance.

Determining the friction inside the system

The previous formulas are used for determining the friction in the annulus as well as at the entrance of the tank. Using the previous equations, the total friction e_{diss} in formula (2.2) can be replaced with the following formula.

$$e_{diss} = f \frac{h(t)}{D_h} \frac{1}{2} v(t)^2 + K_{tot} \frac{A_{an}^2}{A_{en}^2} * \frac{1}{2} v(t)^2 \tag{2.25}$$

Where $f[-]$ equals the given Darcy-Weisbach friction factor, which depends on the Reynolds number of the fluid. The first part of the right term stands for the loss through friction in the annulus, where the second part stands for the dissipation of energy due to the entrance(s) of the tank.

2.2 The mechanical energy balance for the insulation tank

With the new information, formula (2.2) can be rewritten by using formulas (2.9), (2.18) and (2.25) and the assumptions made in section (2.1). This is put together and divided by the mass flow from formula (2.19).

$$\frac{1}{2} v(t)^2 + h(t) \frac{dv(t)}{dt} + gh(t) = gH - f \frac{h(t)}{D_h} \frac{1}{2} v(t)^2 - K_{tot} \frac{A_{an}^2}{A_{en}^2} * \frac{1}{2} v(t)^2 \tag{2.26}$$

Rewriting this formula gives the following.

$$\frac{dv(t)}{dt} = g \frac{H}{h(t)} - g - \frac{1}{2} \frac{v(t)^2}{h(t)} - \frac{f}{D_h} \frac{1}{2} v(t)^2 - K_{tot} \frac{A_{an}^2}{A_{en}^2} * \frac{1}{2} \frac{v(t)^2}{h(t)} \tag{2.27}$$

Together with formula (2.5), this is the final solution for the mechanical energy balance inside the insulation tank. Here can be seen that the pressure is the driving force of the water flow, and the increase in potential energy, kinetic energy and losses due to friction slow down the buildup of velocity.

2.3 Numerical approach

2.3.1 Discrete and continuous time

In the numerical model discrete time steps are used, instead of the continuous time calculations made this far. Therefore, calculations become a little bit different from the exact continuous time solution. When the determined time step Δt is small enough calculations become quite accurate. In discrete time the height and velocity are written as follows.

$$v(t) = v_n \tag{2.28}$$

$$h(t) = h_n \tag{2.29}$$

The system is calculated in steps of n. Therefore time t can be determined by n.

$$t = n * \Delta t \tag{2.30}$$

Some of the relations given change something. First, the velocity over time changes. With the translation to discrete time, for a time step Δt small enough, the Euler method can be used to approximate the derivatives of $v(t)$ as well as $h(t)$. This gives the following.

$$\frac{dv(t)}{dt} = \frac{v_{n+1} - v_n}{\Delta t} \tag{2.31}$$

There is no change in dimensions. v_n is still in $[\frac{m}{s}]$. Secondly, the height differentiated over time changes and therefore it's relationship with $v(t)$ as well.

$$\frac{dh(t)}{dt} = \frac{h_{n+1} - h_n}{\Delta t} = v_n \tag{2.32}$$

Here the dimensions do not change either. It is important to notice this is an example for the explicit solution. When solving the equation implicitly, the last term of equation (2.32) becomes v_{n+1}. This is further explained in section (3.1). Because many terms on the right side of the equation are divided by $h(t)$, there occurs a problem in the boundary conditions using discrete time. With $h(0) = 0$ at $t = 0$ this formula will give an infinite acceleration, but that infinite acceleration holds only for an infinite small amount of time. The problem is solved to give an initial velocity to the water flow for a small amount of time and as a result also give an initial height. This get further explanation in section (3.2).

2.3.2 First order Taylor expansion

To be certain of a stable result, a first order Taylor expansion of the function is used. The stability of the result guaranteed because the first order expansion linearizes the function. The first order Taylor expansion gives the value and slope at a certain point a or b of the function. By calculating the first order Taylor expansion at point h_n, the value at h_n, as well as the slope is given. As a result a good approximation of h_{n+1} can be made when the time step Δt is small enough. The definition of the first order Taylor expansion for a formula with two variables is as follows.

$$f(x, y) \approx f(a, b) + f'_x(a, b)(x - a) + f'_y(a, b)(y - b) \tag{2.33}$$

The approximation only holds for just small differences between x and a and y and b, which is the case when a small Δt is taken. In formula (2.27), there are thee different functions that must be written out as a first order Taylor expansion. These are the following.

$$\frac{1}{h_{n+1}} \approx \frac{1}{h_n} - \frac{1}{h_n^2}(h_{n+1} - h_n) \tag{2.34}$$

$$v_{n+1}^2 \approx v_n^2 + 2v_n(v_{n+1} - v_n) \tag{2.35}$$

$$\frac{v_{n+1}^2}{h_{n+1}} \approx \frac{v_n^2}{h_n} - \frac{v_n^2}{h_n^2}(h_{n+1} - h_n) + 2\frac{v_n}{h_n}(v_{n+1} - v_n) \tag{2.36}$$

2.4 Decay heat inside the reactor vessel

It is of large importance for the safety of the SLIMR that it keeps the ability to cool itself passively. The cooling process of a reactor with insulation tank differs greatly from a reactor without insulation tank. To determine whether further research on the insulation tank is useful, an attempt has been made to approximate the buildup of heat inside the reactor during the filling of the tank. Therefore, first the decay heat inside the reactor has to be known. Veling [3] proposed a formula for the decay heat after SCRAM is initiated inside the reactor. This formula is the following.

$$P_{heat}(t) = 6.48 * 10^{-3}((\frac{t}{86400})^{-0.2} - ((\frac{t}{86400} + T_0)^{-0.2}) * P_0 \tag{2.37}$$

In this formula, $P_{heat}[\frac{J}{s}]$ is the heat generated by the decaying isotopes inside the reactor core. $t[s]$ is the time after shutdown of the reactor. T_0 is the total operation time in days the reactor is running and P_0 is the nominal power production before shutdown. Formula (2.37) shows the generated heat at a particular point in time. To get the total increase in heat energy during the filling time, formula (2.37) is integrated over discrete time.

$$E_{heat} = \sum_{n=0}^{n_{half}} P_n * \Delta t = \sum_{n=0}^{t/2} \Delta t * 6.48 * 10^{-3}((\frac{t_n}{86400})^{-0.2} - ((\frac{t_n}{86400} + T_0)^{-0.2}) * P_0 \quad (2.38)$$

In this case $E_{heat}[J]$ is the total heat energy that is put into the system due to decaying atoms. While the insulation tank is filling, the cooling process already is ongoing. For this research half the filling time is approximated as the time needed before the cooling process begins, therefore the sum in formula (2.38) is taken from $n = 0$ to n_{half}, which the amount of steps needed to get to half the filling time.

$$n_{half} = \frac{t_{fill}}{2\Delta t} \quad (2.39)$$

After the half of the time the filling process is not finished, but more than half of the insulation tank is filled and therefore the cooling process already is started. Besides, because the water now flows over the reactor pressure vessel the cooling is expected to be more efficient during the filling than when the water was stagnant. As a result, taking half the filling time seems a fair and even somewhat conservative estimate of reality.

2.5 Temperature increase

This decay heat results in an increase in temperature inside the reactor before the cooling process starts. The goal of this section is to be able to approximate the increase in temperature while the insulation tank is being filled. Two different methods of calculating the temperature increase are done. It is important to notice that the pressure is assumed to be constant on $25[MPa]$: only the increase in temperature is calculated. The first method uses the density and heat capacity of the water at two different states: the first is the state inside the core and the riser and uses the outlet temperature of the core, the second state is in the rest of the reactor and uses the inlet temperature of the reactor. This is the left example in figure (2.2). The second method approximates the average density and specific heat capacity over the range of temperature of the water inside the tank, shown in the right side of figure (2.2). In both methods there is a percentage of metal inside the reactor taken into account to cover the heat capacity of the structure of the riser and the core. The temperature increase of the reactor pressure vessel is put out of the scope of this research to keep the result conservative. Namely, part of the decay heat is absorbed into the RPV. There are a few things worth noticing. One is that the decay heat is divided equally over the reactor. This approximation is done because during the filling of the insulation tank the mass flow inside the reactor is hardly decreased. Secondly, the heat loss to the heat exchanger is not taken into account.

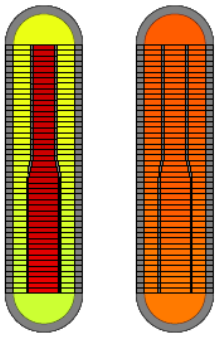

Figure 2.2: Examples of the two different methods used for heat calculations.

Heat capacity and density

The goal of both methods is to calculate the total heat capacity of all materials inside the reactor. Using the heat capacity, density and the increase in heat energy given in formula (2.38), the temperature increase can be calculated. To determine the heat capacity and density of the water

inside the reactor the properties of the supercritical water are needed. These are found in the research of Pioro et al.[8], given in figure (2.3). These figures are used as well as the tables in the Transport Phenomena Data Companion[9] for the material properties.

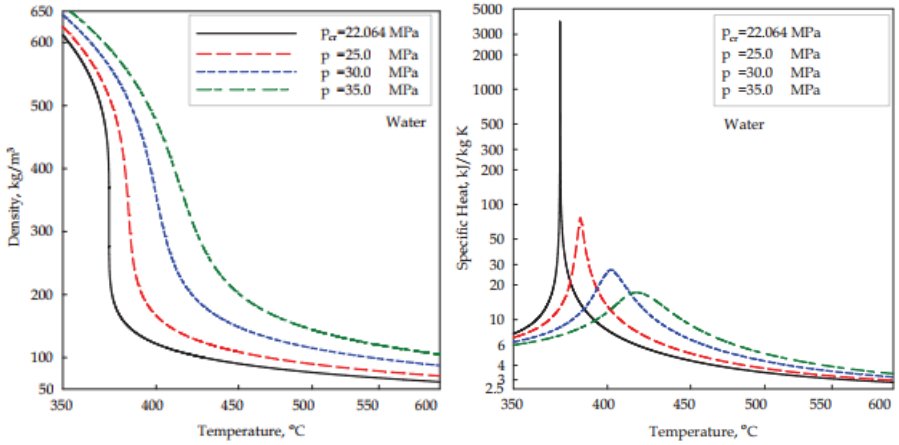

(a) Density of water over temperature for different pressures.

(b) Specific heat capacity over temperature for different pressures

Figure 2.3: Graphs showing (a) the density and (b) the specific heat for different temperatures and pressure. In this research the 25$[MPa]$ graph is of our interest. Data from I. Pioro [8]

Volume inside the reactor

To calculate the heat capacity, the inner volume of the reactor pressure vessel must be known, the RPV itself in not included. This is a part cylinder and at the top and bottom a hemisphere, as is shown in figure (1.1). Adding these gives the following reactor volume.

$$V_{reactor} = (L - D_{rpv,out})\frac{\pi D_{rpv,in}^2}{4} + \frac{4\pi}{3}D_{rpv,in}^3 \tag{2.40}$$

The length of the cylinder is the total length of the reactor, $L[m]$, minus the outer diameter of the RPV $D_{rpv,out}[m]$. Because only the inner volume of the RPV is calculated the rest of the calculations are done with $D_{rpv,in}[m]$ [3].

2.5.1 Method 1: Density and heat capacity at core inlet and outlet temperature

The first method describes the situation inside the reactor as having the core and riser filled with water at core outlet temperature, and having the rest of the reactor filled with water at core inlet temperature. Because the different temperatures of the water, there is also a difference in heat capacity and density. Using the ratio of the volume inside the core and riser and the rest of the volume, a total heat capacity inside the RPV is calculated. Multiply that by the heat energy generated during half the filling time gives an approximation of the increase in temperature, given in formula (2.42). Therefore, for the first method not only the total volume of the reactor is needed but also the volume inside the core and riser [3] [5]. This is a very straightforward calculation.

$$V_{CR} = \frac{\pi}{4}(L_{riser}D_{riser}^2 + L_{core}D_{core}^2) \tag{2.41}$$

Here $V_{CR}[m^3]$ is the volume of the riser and the core, $L_{riser}[m]$ and $D_{riser}[m]$ the length and the diameter of riser, and so are $L_{core}[m]$ and $D_{core}[m]$ the length and diameter of the core.

Using V_{CR} and $V_{reactor}$, the ratio of the volume containing water at core outlet temperature and water at core inlet temperature is known. After the heat capacities and densities of the water at the two different temperatures and that of the stainless steel are determined, the temperature difference can be calculated as follows.

$$\Delta T_1(t) = E_{heat} * (V_{reactor}((1 - \%_{st})(c_1\rho_1\frac{V_{RC}}{V_{reactor}} + c_2\rho_2\frac{V_{reactor} - V_{RC}}{V_{reactor}}) + \%_{st}c_{st}\rho_{st}))^{-1} \quad (2.42)$$

Here $\Delta T(t)[K]$ is the change in temperature over time. $\%_{st}$ is the percentage of the total volume that consists of steel. $c_1[\frac{kJ}{kgK}]$ and $\rho_1[\frac{kg}{m^3}]$ are the specific heat capacity and density of the fluid inside the riser and core of the reactor. The specific heat capacity and density with subscript 2 are the values for the fluid in the rest of the reactor, while subscript *st* is for the steel inside the reactor.

2.5.2 Method 2: Averaged density and heat capacity over the range between core inlet and outlet temperature

For the situation where the temperature is evenly distributed over the reactor the equation is the following.

$$\Delta T_2(t) = E_{heat} * (V_{reactor}((1 - \%_{st})c_{avg}\rho_{avg} + \%_{st}c_{st}\rho_{st}))^{-1} \quad (2.43)$$

In this equation $c_{avg}[\frac{kJ}{kgK}]$ and $\rho_{avg}[\frac{kg}{m^3}]$ are the approximated average specific heat and density in the range between the inlet and outlet temperature given in the research of Krijger [5]. Chosen is to take the average over the range because in figure (2.3) can be seen that the heat capacity and the density have very large fluctuations over the range worked with. During normal operation these density fluctuations are very beneficial for the mass flow.

Chapter 3

Numerical models and methods

The numerical models in this research are based on the theory in Chapter (2). The goal of the numerical model is that the solutions for the mechanical energy balance, formula (2.5) and (2.27), represent the physics with a right code in MatLab [10]. Therefore, first in section (3.1) the explicit and implicit methods are given. Secondly, in section (3.2) the right boundary conditions and starting conditions are determined. Thirdly, in section (3.3) the geometrical factors determining the filling time are treated and a prediction is made how they influence the system. In section (3.4) the experimental method and flowcharts of the scripts are given. Finally, in section (3.5) the decay heat calculations are given.

3.1 Explicit and implicit method

There are two possibilities to discretize the differential equation. The first solution is to solve the equation explicitly. The explicit method uses the solution on the current time step to calculate the state of a system in the next time step. In other words, v_{n+1} and h_{n+1} are calculated by using v_n and h_n. The implicit method, on the other hand, uses both the current and next time step to calculate the state of the system in the next time step. Both methods are discussed separately. In section (4.2), the solutions will be compared.

3.1.1 Explicit method

The explicit method uses the current time step to calculate the following time step. The explicit solution however can become unstable. To overcome this, the time step must become very small which extends the calculation time. First, the explicit solution for the mechanical energy balance is given and rewritten.

$$\frac{v_{n+1}-v_n}{\Delta t} = \frac{gH}{h_n} - g - \frac{1}{2}\frac{v_n^2}{h_n} - \left(\frac{1}{-1.8log_{10}(\frac{6.9\mu}{\rho_w v_n D_h})}\right)^2 \frac{1}{D_h}\frac{1}{2}v_n^2 - K_{tot}\frac{A_{an}^2}{A_{en}^2} * \frac{1}{2}\frac{v_n^2}{h_n} \tag{3.1}$$

Which is rewritten for v_{n+1}.

$$v_{n+1} = v_n + \Delta t\left(\frac{gH}{h_n} - g - \frac{1}{2}\frac{v_n^2}{h_n} - \left(\frac{1}{-1.8log_{10}(\frac{6.9\mu}{\rho_w v_n D_h})}\right)^2 \frac{1}{D_h}\frac{1}{2}v_n^2 - K_{tot}\frac{A_{an}^2}{A_{en}^2} * \frac{1}{2}\frac{v_n^2}{h_n}\right) \tag{3.2}$$

Our solution for the mechanical energy balance is an equation that is potentially unstable, because it is almost in every term divided by h_n. In section (4.2) is shown that indeed the explicit solution can become unstable and is therefore not sufficient for all calculations in this project. h_{n+1} is calculated using by:

$$\frac{h_{n+1}-h_n}{\Delta t} = v_{n+1} \tag{3.3}$$

Rewrite this for h_{n+1} gives the following.

$$h_{n+1} = h_n + v_{n+1} * \Delta t \tag{3.4}$$

3.1.2 Implicit method

With the knowledge that the explicit method may not be stable for the whole range of geometries used in this project, also the implicit method is used. This method needs more computation, since matrix inversion is required, but the advantage of this method is that it is inherently stable. The first step is writing the mechanical energy solution at $n+1$.

$$\frac{v_{n+1} - v_n}{\Delta t} = \frac{gH}{h_{n+1}} - g - \frac{1}{2}\frac{v_{n+1}^2}{h_{n+1}} - (\frac{1}{-1.8log_{10}(\frac{6.9\mu}{\rho_w v_n D_h})})^2 \frac{1}{D_h}\frac{1}{2}v_{n+1}^2 - K_{tot}\frac{A_{an}^2}{A_{en}^2} * \frac{1}{2}\frac{v_{n+1}^2}{h_{n+1}} \tag{3.5}$$

Now all $n+1$ terms on the right hand side can be approximated using terms in current time n as shown in section (2.3.2). Notice that the velocity term in the *log* function is written as v_n. This is because this term has a small effect on the system and at the same time hard to rewrite linearly. Thereby this function is linearized for v_{n+1} and h_{n+1}. This is done and the function is rewritten. This gives the following.

$$v_{n+1} = v_n + h_{n+1}\Delta t(-\frac{gH}{h_n^2} + \frac{K+1}{2}\frac{v_n^2}{h_n^2}) + v_{n+1}\Delta t(-(K+1)\frac{v_n}{h_n} - (\frac{1}{-1.8log_{10}(\frac{6.9\mu}{\rho_w v_n D_h})})^2 \frac{v_n}{D_h}) + \Delta t(\frac{2gH}{h_n} - g + (\frac{1}{-1.8log_{10}(\frac{6.9\mu}{\rho_w v_n D_h})})^2 \frac{1}{2D_h}v_n^2 \tag{3.6}$$

The result for h_{n+1} is not different than using the explicit method. Therefore formula (3.4) can be used. These functions are written in the following matrix form.

$$\boldsymbol{A}\vec{\boldsymbol{x}} + \vec{\boldsymbol{b}} = \vec{\boldsymbol{x}} \tag{3.7}$$

The result is shown below.

$$\begin{bmatrix} 0 & \Delta t \\ \Delta t(-\frac{gH}{h_n^2} + \frac{K+1}{2}\frac{v_n^2}{h_n^2}) & -\Delta t((K+1)\frac{v_n}{h_n} + \frac{f}{D_H}v_n) \end{bmatrix} \begin{bmatrix} h_{n+1} \\ v_{n+1} \end{bmatrix} + \begin{bmatrix} h_n \\ v_n + \Delta t(\frac{2gH}{h_n} - g + \frac{f}{2D_H}v_n^2) \end{bmatrix} = \begin{bmatrix} h_{n+1} \\ v_{n+1} \end{bmatrix} \tag{3.8}$$

The matrix form in formula (3.7) can be rewritten so $\vec{\boldsymbol{x}}$ is given. The calculations a as follows.

$$\vec{\boldsymbol{x}} = -(\boldsymbol{A} - \boldsymbol{I})^{-1} * \vec{\boldsymbol{b}} \tag{3.9}$$

Where $\boldsymbol{I}$ is the identity matrix. For the mechanical energy balance this calculation is done by MatLab.

3.2 Determining the boundary conditions and beginning of the flow

For the explicit as well as the implicit solution the first steps of the process are crucial, because the acceleration is very large in the beginning. In fact, because $h_0 = 0$ using our intentional boundary conditions the acceleration at $t = 0$ is infinite. To overcome this, the system is given an increment velocity at the first step and from that velocity an increment height is calculated. This increment velocity is determined by again using the mechanical energy balance (2.27) and multiply this equation with $h(t)$.

$$h(t)\frac{dv(t)}{dt} = gH - gh(t) - \frac{1}{2}v(t)^2 - \frac{fh(t)}{D_h}\frac{1}{2}v(t)^2 - K_{tot}\frac{A_{an}^2}{A_{en}^2} * \frac{1}{2}v(t)^2 \tag{3.10}$$

The left side of the equation is now set at $n = 1$ where the right side of the equation is at point $n = 0$. Both h_0 as well as v_0 is zero, thereby the following is left of the equation.

$$h_1 \frac{v_1}{\Delta t} = gH \tag{3.11}$$

Using formula (3.4) to rewrite h_1 in terms of v_1 a result for v_1 can be found.

$$v_1 = \sqrt{gH} \tag{3.12}$$

Putting the result for v_1 back in formula (3.4) also a result for h_1 is found.

$$h_1 = \sqrt{gH} * \Delta t \tag{3.13}$$

For the explicit solution, this is potentially a good solution to overcome the unstable behavior of the equation. Only, for too large as well as to small values of Δt, stability problems still exist. First, when Δt becomes too large, there is a significant initial starting height, which is wanted. But when Δt becomes too large in formula (3.2), v tends to have large changes. The corrections to these changes also tend to become too large, thereby making the solution unstable. For the implicit solution these problems do not tend to occur. Because of the linearity of the equation with respect to v_{n+1} and h_{n+1}, the smaller the time step the better the approximation.

3.3 Different geometries

The goal of this research is to determine the filling speed of the insulation tank, as well as the influence of the geometrical factors playing a role in this process. The influential factors are the depth of the tank inside the pool, H, the diameter of the annulus cylinder D_{an}, the cross-sectional area of the entrance A_{en} and the inlet friction coefficient K. For these four factors is examined how the filling time changes if the each factor is independently varied.

The depth, the entrance cross-sectional area and the friction coefficient are expected to affect the system in the same way. For example, by increasing the depth of the tank in the pool, the height H increases and the force driving the flow increases. This effect can only have positive influence on the system. This also applies to the resistance coefficient K. By lowering the resistance coefficient, for example by making the entrance straight instead of giving the entrance tube angles, the friction on the system lowers and consequently the filling time lowers. The same applies for increasing the entrance cross-sectional area. Increasing the cross-sectional area of the entrance reduces the resistance quadratically. It is expected that the depth of the reactor inside the pool has the least influence on the filling time, because the changes, $0[m]$ to $5[m]$ depth, are small with respect to the driving force of the pressure due to the length of the reactor, $16.4[m]$.

Changing the inner diameter of the outer cylinder may be not that straightforward as the other two are. By changing the dimensions of the annulus not only the entrance friction changes, but also the wall friction inside the pipe changes because of the changing hydraulic diameter. Expected is that the effect of the changing hydraulic diameter in this project is negligible, because the annulus worked with is at least a few centimeters.

3.4 Numerical setup

Both the explicit and implicit models will be used in this experiment. Comparing both methodologies, a decision is made whether to continue with one or the other model for the rest of this project. This decision is made on accuracy, stability and calculation time.

3.4.1 The flowchart of the explicit model

The flowchart of this model is given by figure (3.1). First, the parameters that keep constant during the calculations are given. Then, the initial conditions are set. In this case the initial conditions are the values of v_0, h_0, v_1 and h_1 as explained in section (3.2). After the constants and initial conditions are given, the time stepping loop begins. This loop is first calculating the velocity of the next time step. Using this velocity a new height is calculated. This loop continues till the insulation tank is full. When the tank is full the loop ends and the data of the velocity, height and total filling time are obtained.

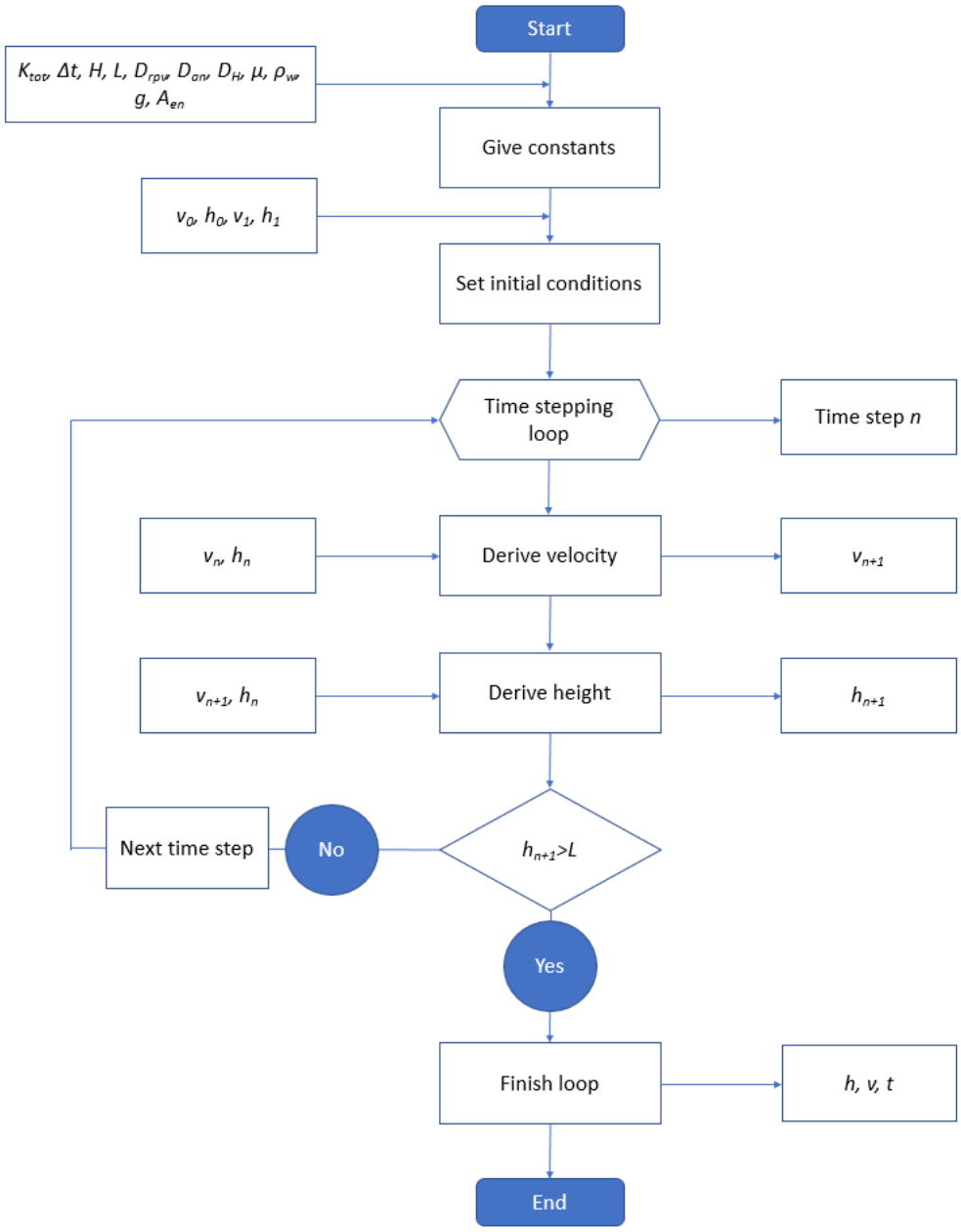

Figure 3.1: A flowchart of the steps taken and input of information in MatLab to calculate the velocity and height of the water in the insulation tank while solving the mechanical energy balance explicitly.

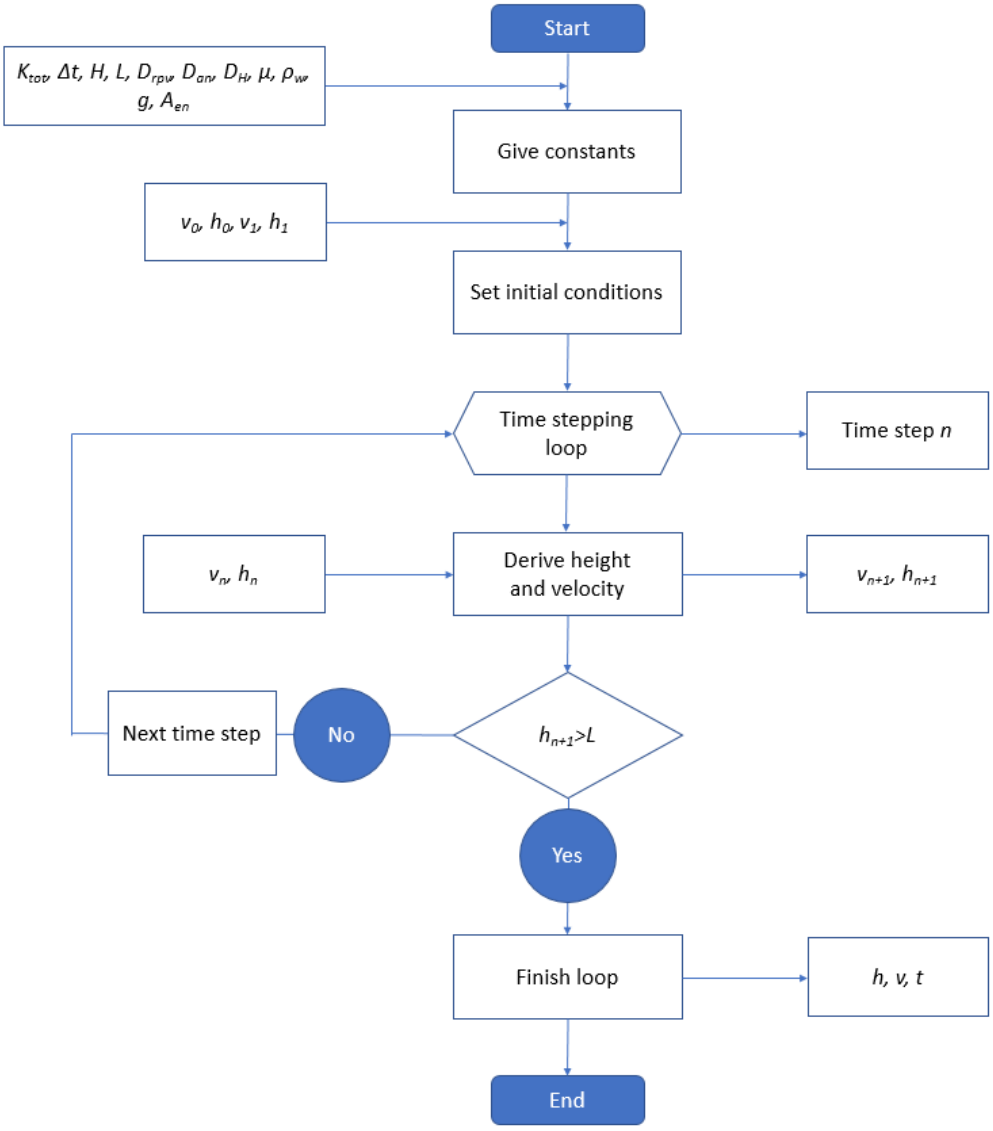

Figure 3.2: A flowchart of the steps taken and input of information in MatLab to calculate the velocity and height of the water in the insulation tank while solving the mechanical energy balance implicitly.

3.4.2 The flowchart of the implicit model

Since the implicit model does not differ that much from the explicit model only the differences will be discussed. The steps before the time stepping loop are equal to the flowchart of the explicit method. Inside the flowchart the velocity as well as the height are derived at the same moment. The flowchart of the implicit model is shown in figure (3.2)

3.5 Decay heat and temperature increase

The calculations for the decay heat are given in section (2.4). In this section the approximations done are discussed. Before devoting to the two approximation methods, first shortly total operation time in days the reactor is running and the percentage of steel inside the reactor and its characteristics are discussed. According to Veling [3], the total operation time is days hardly influences the decay heat in the first hour after SCRAM is initiated. Therefore, $T_0[days]$ is chosen at $5000[days]$ to be sure that our approximation is rather to high than too low. The percentage of steel (the core, riser and constructional steel) is approximated at 20%. The density of stainless steel is determined at $7700[\frac{kg}{m^3}]$, the heat capacity of steel over the different temperatures is

approximated as $0.46[\frac{kJ}{kgK}]$.

3.5.1 Method 1: Density and heat capacity at core inlet and outlet temperature

The first situation is using different temperatures in the riser and core and the rest of the reactor. Therefore, at the two points the specific heat capacity and density are approximated. According to Krijger [5], the core outlet temperature is $396[^\circ C]$. Out of the graphs of figure (2.3) the density with given temperature and pressure is approximated at $170[\frac{kg}{m^3}]$. The specific heat capacity is approximated at $14[\frac{kJ}{kgK}]$. Both factors are chosen conservatively, because preferred is to get a too high result over a result that is too low. The inlet temperature in Krijger is determined in the range of $280 - 290[^\circ C]$. Because this is out of the range of the graph the tables of the Transport Phenomena Data Companion [9] are used. The density is approximated at $700[\frac{kg}{m^3}]$. The specific heat capacity for the same reason is determined at $5[\frac{kJ}{kgK}]$. This is an extrapolation of the graphs but mainly the known value out of the tables.

3.5.2 Method 2: Averaged density and heat capacity over the range between core inlet and outlet temperature

The second solution is made by approximating the average values of the density and the specific heat capacity over the range of temperatures worked with. Therefore the same information as for the first solution is taken and the graphs of figure (2.3) are extrapolated in combination with the known values out the tables [9]. The supercritical water reaches a maximum heat capacity of $76[\frac{kJ}{kgK}]$. But, taking a high heat capacity could make the approximation too positive and it is expected that there is small percentage of the water has this high heat capacity. Taking this into account the average specific heat capacity is approximated at $6[\frac{kJ}{kgK}]$. The density is determined with the same reasoning at $550[\frac{kg}{m^3}]$.

Chapter 4

Results

The results consist of an introduction giving the basic dimensions of the reactor and insulation tank. This is discussed in section (4.1). After the introduction the differences in the results for the explicit and implicit solutions are discussed in section (4.2). After the best solution is chosen, the effects of changing each dimension independently are given in section (4.3). In section (4.4) the temperature increase before the beginning of the cooling is determined. Finally, a practical geometry for the insulation tank is proposed in section (4.5).

4.1 Basic dimensions of the insulation tank geometry

For each calculation just one factor determining the geometry is changed, so that the change in filling time for each different factor can be isolated. To compare the calculations changing different geometrical factors a basic dimension of the tank is given in table (4.1). The dimensions of the reactor are from the report of Veling [3].

In figure (2.1) a simple schematic drawing of the insulation tank was shown. With the basic dimensions and the results of section (4.2) for the time step the total filling time is 12.04$[s]$

Geometry dimensions	Name	Value
Deepest point of insulation tank	H	$18.4m$
Length of the insulation tank	L	17.4
Outer diameter annulus	D_{an}	$4.2m$
Outer diameter reactor	D_{rpv}	$3.2m$
Depth in pool	$Depth$	$1m$
K value	K	2
Entrance cross-sectional area	A_{en}	$1m^2$

Table 4.1: Table with the standard geometry of the tank. For each measurement just one parameter is differed.

In figure (4.1) the graphs are shown for the solution of the filling of the insulation tank for the standard geometrical dimensions as indicated in table (4.1). Figure (4.1b) shows the velocity over time for the basic dimensions. The initial velocity $v(0)$ for the standard dimensions of 13.44$[\frac{m}{s}]$, calculated with formula (3.12). When $h(t)$ increases the driving force decreases while the friction forces increase. As a result the velocity decreases to around 2$[\frac{m}{s}]$, with a small decrease over time. When the height of the water increases the pressure due to height differences decreases. Consequently velocity decreases. It is important to notice that during the process the surface of the annulus as well as the hydraulic diameter are determined on their values in the annulus. In other words, the spherical shape at the top and bottom are not included in the calculations.

4.2 Explicit versus implicit solution

To check whether the explicit and implicit solutions are possible correct approximations of the solution to the mechanical energy balance they are compared. All the stable results are given in

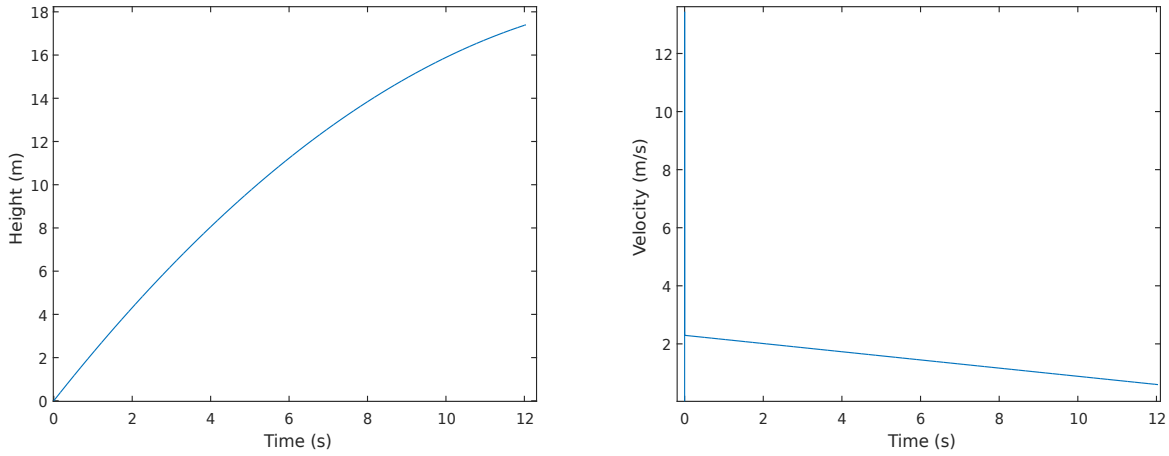

(a) Height $h(t)$ versus time

(b) Velocity $v(t)$ versus time

Figure 4.1: Graphs showing (a) the height and (b) the velocity of the water inside the insulation tank given the standard geometry

figure (4.2). Because of the instability of the explicit result, in this figure results are given where the first step as in formula (3.13) is done with a Δt of $0.1[s]$, after which the rest of the calculations are done with the Δt value shown at the x-axis. Making this initial time step larger makes the total process faster than it really is, because after the initial time step the velocity decreases. To still be able to compare the explicit and implicit solution the implicit solution in this graph also has an initial time step of $0.1[s]$. As can be seen in this figure, for a smaller time step the result of the explicit solution approaches the result of the implicit solution. In section (4.2.2) the implicit result is given without using a different Δt as the initial time step relative to the rest of the calculations. Because the implicit solution has no stability problems and an acceptable calculation time chosen is to work with the implicit solution during the rest of the project.

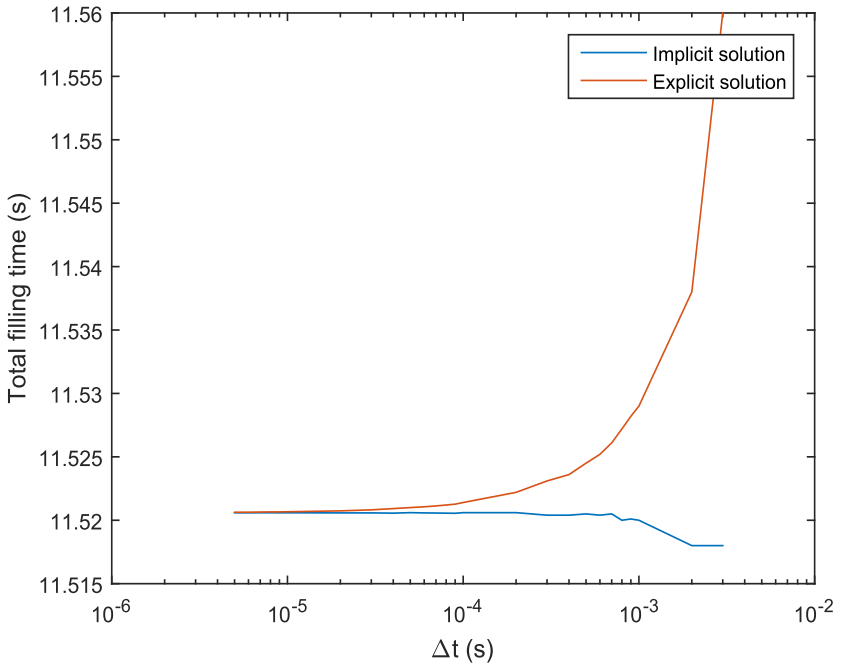

Figure 4.2: Graph comparing the explicit and implicit solution of the total filling time for different values of Δt. All the first steps have the same Δt value of $0.1[s]$.

4.2.1 Explicit solution

Having a too large Δt, the explicit solution becomes unstable. This is shown in figure (4.3), the results with for Δt is larger than $0.003[s]$ the equation is instable and after a few steps the height reaches unrealistic high values. This is shown in figures (4.3b) and (4.3c). When no difference is made between the time of the initial step and the Δt, the explicit solution becomes unstable for too small values of Δt. This is because for a small initial time step $h(0) << 1$.

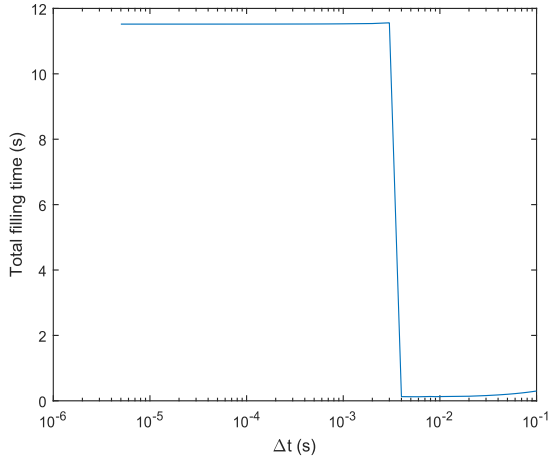

(a) All explicit results of total filling time

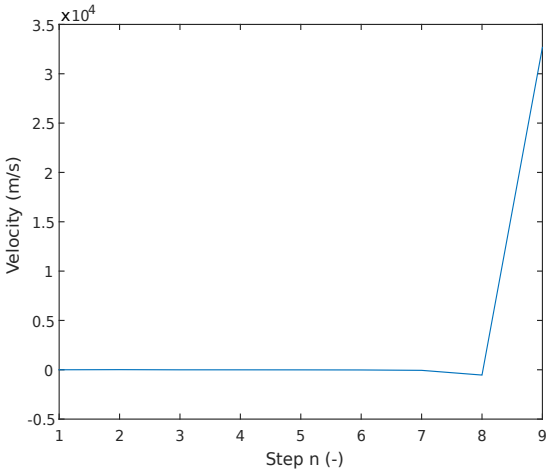

(b) Velocity per step

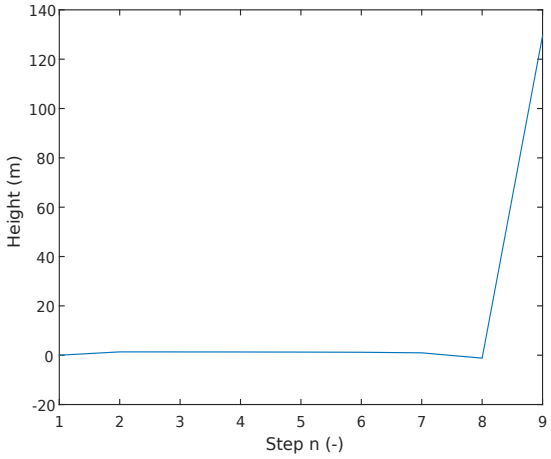

(c) Height per step

Figure 4.3: Graphs showing (a) the explicit solution for different values of Δt with a first step of $0.1[s]$, (b) the velocity per step of an instable result and (c) the height per step of an instable result. For (b) and (c) the time step is $0.004[s]$.

4.2.2 Implicit solution

The implicit solution has a result for every Δt. The result for the implicit solution without the initial Δt of $0.1[s]$ is given in figure (4.4). With the implicit method it is possible to take a smaller time step for the initial step. This makes the approximation more accurate because the initial time step is expected to overestimate the real velocity, since thereafter the velocity of the water decreases. Therefore, the choice is made to do the calculations changing the geometrical factors with the implicit method. Making the time step as small as possible, to lower the effect of the initial time step, and taking in consideration the calculation time of MatLab the chosen time step Δt is set at $10^{-4}[s]$.

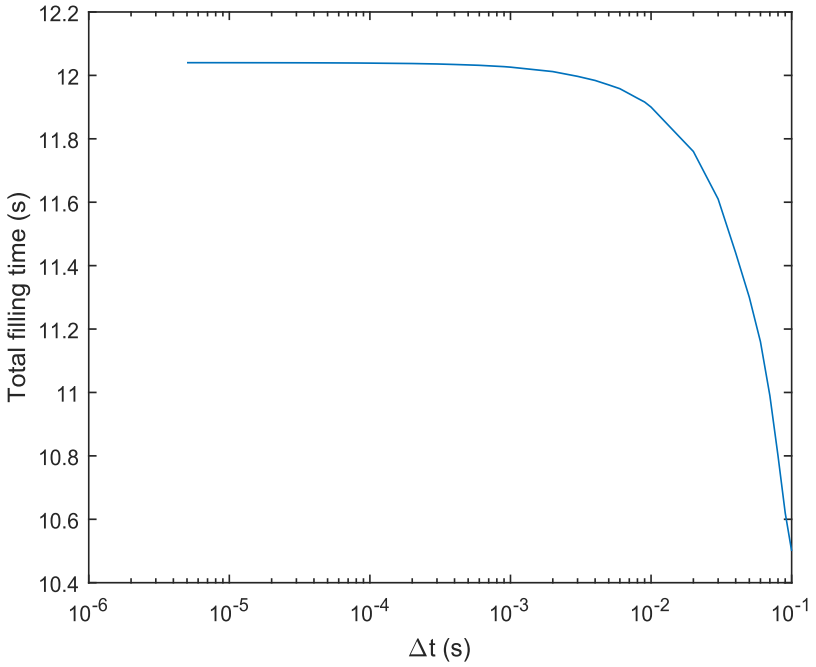

Figure 4.4: Graph showing the implicit solutions of the total filling time per Δt size.

4.3 Changing geometrical factors

Now the filling time with the basic dimensions is given, the geometrical factors affecting the system are changed independently, while measuring the change in filling time. These geometrical factors are the annulus diameter D_{an}, the entrance cross-sectional area A_{en}, the entrance friction K and the depth of the tank into the pool, which in the formula is an element of H. This process and some expectations are discussed in section (3.3). For each of the four a graph is given to show the height over time while taking five different values for this factor. This graph shows the change in the way of flow over time. Also a second graph is given, showing the value of the geometrical factor versus the total filling time. This graph shows how the total filling time depends on this factor. The basic dimensions of table (4.1) are used, except the one factor this is changed. Of the second graph a fit of the line is made for each function. When there are different values wanted these fits can be extrapolated to estimate how it will influence the filling time. Besides, for choosing a practical geometry at the end of the project it is important to know which factor is the most relevant. The function used to fit these relation is as follows.

$$FT(x) = a * x^b + c \tag{4.1}$$

Here FT is the filling time of the insulation tank and x is the value on the x-axis being the factor changed. a, b and c are constants determined by the line and they determine the relation of the geometrical factor to the filling time. This fit shows the dependency of the filling time to each geometrical factor. It is of our interest if the factor has for example an exponential or linear dependency and if this is of large or just small influence.

For each fit the sum of squares due to error (SSE) and the R-square value are given [11]. The SSE value gives the total deviation of the response values from the fit to the given values. The closer the SSE to zero, the better the fit. The R-square method tells how successful the fit explains the variance of the data. A R-square value of 1 means that 100% of the variance is explained by the fit, for a R-square value of zero none of the variance is explained by the fit.

4.3.1 Changing annulus diameter

The graphs for the changing annulus diameter are shown in figure (4.5). As can be seen the total filling time increases for an increasing diameter. In section (3.3) the expectation was that filling

time may increase when $D_{an} \approx D_{rpv}$ (both shown in figure (2.1)). As shown in figure (4.5b) this does not hold for this project. The line in figure (4.5b) is fitted and that resulted in the following.

$$FT(x) = 10.89x^{1.509} + 1.16 \tag{4.2}$$

The SSE for this fit is 1.24 and there is a R-square deviation of 0.9996. These are seen as reasonable results. According to this fit the annulus diameter influences this fit to approximately the power 1.509 ± 0.026. This exponential dependency was expected due to the fact the increasing the diameter quadratically increases the annulus cross-sectional area, A_{an} in formula (2.27). On the other hand the hydraulic diameter D_h increases linearly with increasing annulus diameter and therefore the total friction due to the wall decreases, but the influence of the wall friction is much smaller than the friction of the entrance.

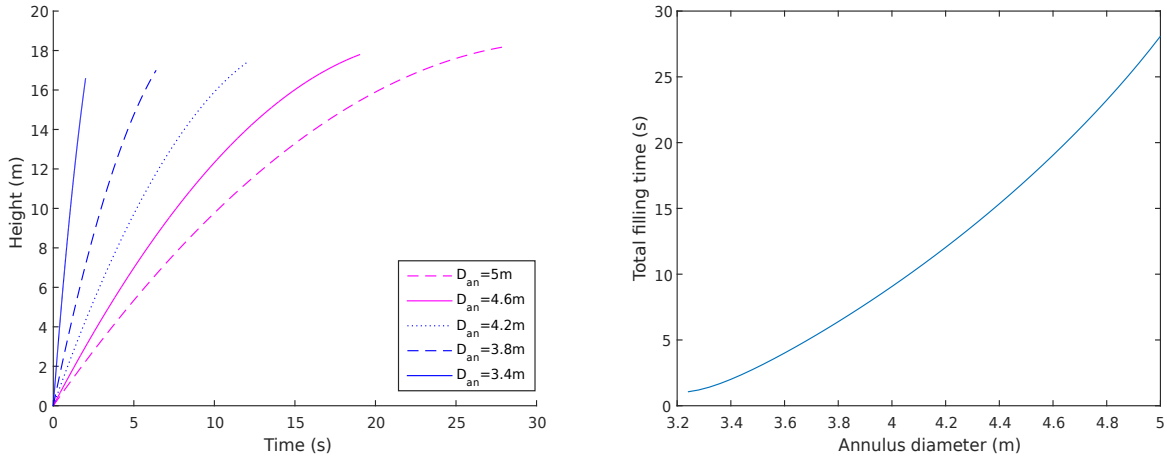

(a) Height graphs

(b) Total filling time

Figure 4.5: Two graphs showing (a) the height for five different outer annulus diameter values and (b) the total filling time by changing the outer annulus diameter.

4.3.2 Changing the entrance cross-sectional area

The results for the filling of the insulation tank with changing entrance cross-sectional area are shown in figure (4.6). As expected an increasing entrance cross-sectional area decreases the total filling time. An increasing area means that the velocity of the water at the entrance relative to the water inside the insulation tank is slower. Therefore, the friction forces at the entrance are of lower and the filling time becomes shorter. In formula (2.27) can be seen that A_{en} is a quadratic term. Increasing the cross sectional area therefore quadratically decreases the friction at the entrance. The line in figure (4.6b) is fitted as follows.

$$FT(x) = 12.34x^{-0.997} - 0.3094 \tag{4.3}$$

The SSE for this fit is 0.001163 and the R-square method gives a value of 1. Therefore this fit is very accurate. The influence of the changing entrance cross-sectional area on the filling time is therefore to the power -0.997 ± 0.0016.

4.3.3 Changing the entrance friction

The friction factor K logically has delaying effect on the total filling time. Increasing the friction at the entrance increases the total filling time. Without any friction the total filling time is $1.08[s]$, which is much shorter than the filling time using the basic geometry of the tank. The curve in figure (4.7b) is fitted as follows.

$$FT(x) = 8.736x^{0.4982} - 0.2993 \tag{4.4}$$

This fit has an SSE of 0.002883 and the value of the R-square is 1. Thus the influence of the inlet friction K to the filling time is to a power 0.4982 ± 0.0008.

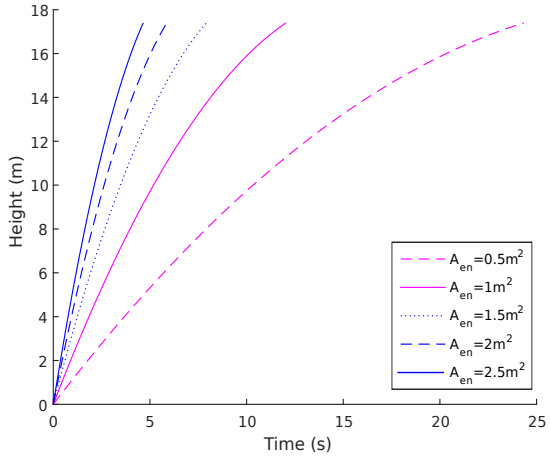

(a) Height graphs

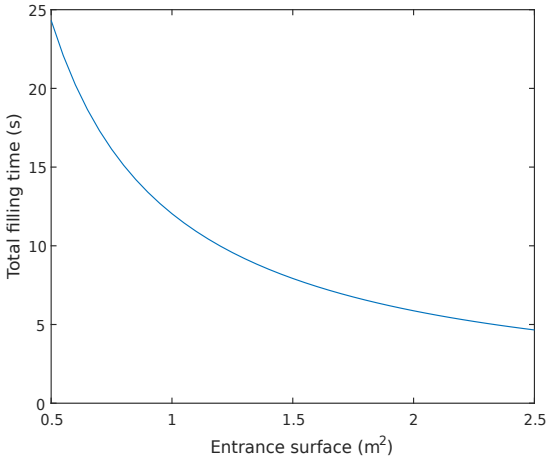

(b) Total filling time

Figure 4.6: Two graphs showing (a) the height for five different relative entrance cross-sectional areas and (b) the total filling time by changing the relative entrance cross-sectional area.

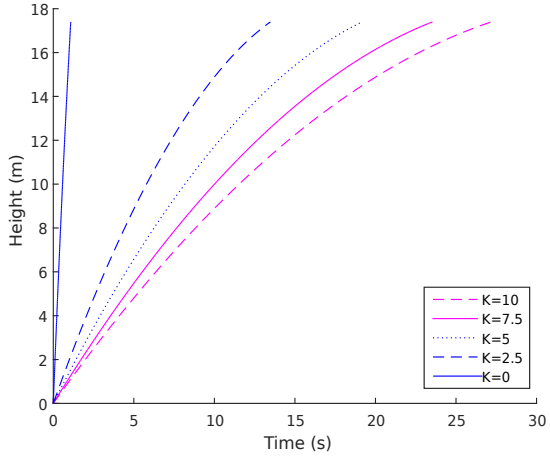

(a) Height graphs

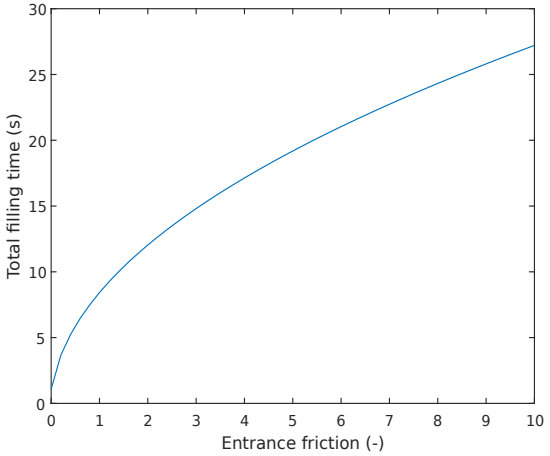

(b) Total filling time

Figure 4.7: Two graphs showing (a) the height for five different values of the friction factor K and (b) the total filling time versus friction factor K.

4.3.4 Changing the reactor depth

The result is in line with our expectation. The deeper the reactor is submerged in the pool, the faster the insulation tank is filled. This is shown in formula (2.27), where a higher depth leads to a higher value for H and as a result an higher driving force of the flow. This is due to the higher pressure on the bottom of the tank. The influence of the reactor depth on the total filling time is determined as follows.

$$FT(x) = -2.577x^{0.4645} + 14.6 \tag{4.5}$$

The SSE of this fit is 0.02319 and the R-square method gives a value of 0.9995. The relation of the depth to the filling time is thereby a power 0.4645 ± 0.0171. Changing the depth has as expected the least influence on the system. Increasing the depth from $0[m]$ to $1[m]$ changes, using the basic dimensions, H from $17.4[m]$ to $18.4[m]$. Therefore it does not have a significant effect on the driving force of the flow.

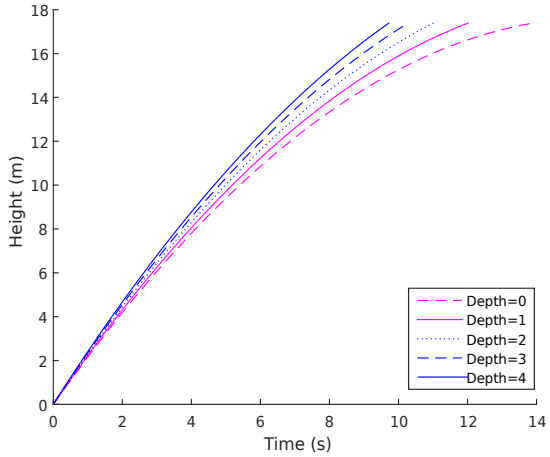

(a) Height graphs

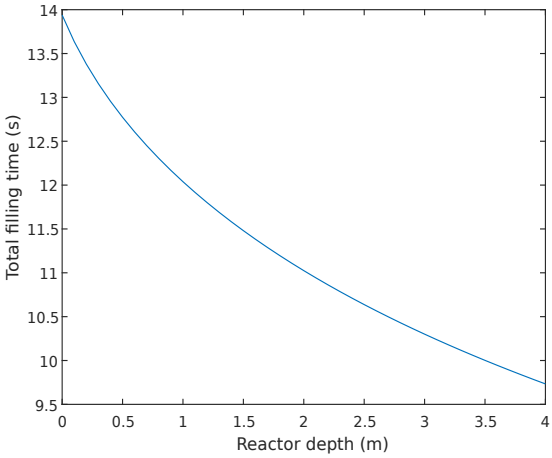

(b) Total filling time

Figure 4.8: Two graphs showing (a) the graphs for five different reactor depths and (b) the total filling time by changing the depth.

4.3.5 Summary

Summarizing most of the expectations in section (3.3) proved to be correct. The annulus diameter does not become so small that the filling time increases. All the constants are summarized in table (4.2). All results are fitted with the same function, shown in formula (4.1). This function is again shown below.

$$FT(x) = ax^b + c$$

This table is made up because it can be used during follow-up study treating the is transfer. By using these fits approximations can be made about the filling time of the insulation tank when geometrical changes are made for the purpose of the heat transfer.

x (Dimensional factor)	a	b	c
Annulus diameter D_{an}	10.89 ± 0.19	1.509 ± 0.026	1.16 ± 0.149
Entrance cross-sectional area A_{en}	12.34 ± 0.02	-0.997 ± 0.0016	-0.3094 ± 0.018
Inlet friction K	8.736 ± 0.024	0.4982 ± 0.0008	-0.2993 ± 0.0248
Reactor depth $Depth$	-2.577 ± 0.11	0.4645 ± 0.0171	14.6 ± 0.11

Table 4.2: Table showing the constants determining the total filling time function for a varying dimensional factor

4.4 Temperature increase

The temperature increase is calculated via two different methods. Using the basic dimensions of the insulation tank given in table (4.1) the increasing heat during half the filling is calculated. For the basic dimensions the result is an increase in temperature of $0.48[K]$ via the method taking two different temperatures. The second method, averaging the density and heat capacity over the range of temperature inside the reactor, the temperature also increases with $0.48[K]$ before the cooling process starts. Both approximations are almost the same. The increase in temperature over time for both solutions is given in figure (4.9). The result of our temperature increase is reasonable.

4.5 Proposing a practical geometry for the insulation tank

Using the basic dimensions, a few possible problems can occur. The first problem is the force the pump must be able to deliver to keep a pressure of approximately $2.8[MPa]$ inside the insulation

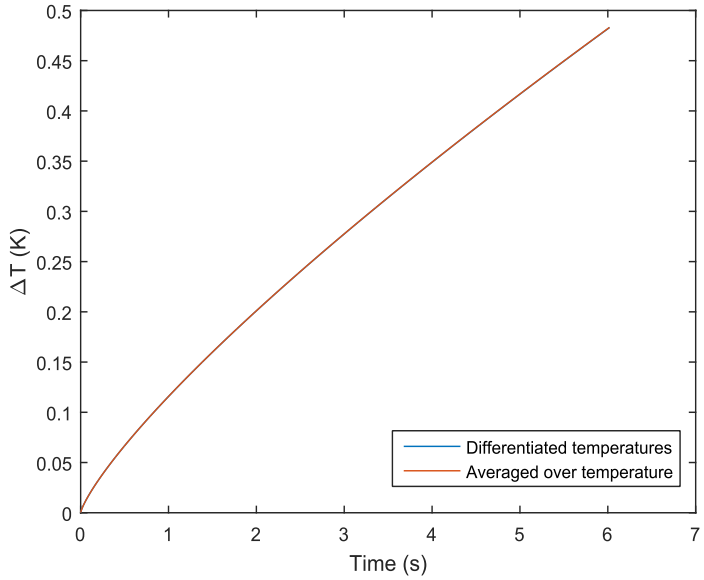

Figure 4.9: The increase of temperature over time inside the reactor during half the filling time of the insulation tank. Both methods have approximately the same result.

tank. With an entrance cross-sectional area of a $1[m^2]$, the force on the entrance is $1.8 * 10^5[N]$. This could mean that a very expensive and energy-consuming pump is needed. A second issue is also a practical one. The outer annulus diameter is now stated at $4.2[m]$. A larger space is beneficial for the insulation of the reactor vessel, but an advantage of the SMR reactors is that they can be made and transported as a whole. Making another stainless steel vessel around it can dispense this advantage. Not only for practical reasons the diameter is made smaller, but this is also beneficial for decreasing the filling time after it has increased by making the entrance cross-sectional area smaller. Temperature increase must be kept as low as possible and therefore a low filling time is required. As shown in figure (4.9) the temperature already increases $0.48[K]$ using the basic dimensions. As a result, the new outer annulus diameter is determined at $3.6[m]$. The value of K is not varied. Because of the friction at the entrance and because of the hemispherical geometry the during the filling a value of $2[-]$ is chosen as a fair number. Also no changes are done to the depth of the reactor. To sink the insulation tank under water for one meter is considered beneficial for losing the heat during the cooling process and speeds up the filling of the insulation tank. Sinking the reactor deeper does not decrease the filling time rapidly and it may be that the pool must be made deeper to fulfill this. Therefore, a final geometry is proposed in table (4.3).

Geometry dimensions	Name	Value
Deepest point of insulation tank	H	$18.4m$
Length of the insulation tank	L	$17.4m$
Outer diameter annulus	D_{an}	$3.6m$
Outer diameter reactor	D_{rpv}	$3.2m$
Depth in pool	$Depth$	$1m$
K value	K	2
Entrance cross-sectional area	A_{en}	$0.5m^2$

Table 4.3: Table with the final proposed geometry of the insulation tank.

The filling time of the insulation tank with the proposed geometry is $8.14[s]$, which is faster than the $12.04[s]$ using the basic dimensions. During this filling time the temperature increases $0.35[K]$ using the first method as well as using the second method. This approximated temperature increase is reasonable and therefore it can be argued that follow-up research would be interesting.

Chapter 5

Conclusions and recommendations

After the initial research on the SLIMR by Rohde [4], Veling [3] and Krijger [5], recommended was to do follow-up research about the heat loss of the reactor during normal operation. The proposal of Krijger was to research the feasibility of an insulation tank around the reactor. This research is the first exploration of the filling time and heat increase inside the reactor during the filling of the insulation tank.

5.1 Conclusions

The most important conclusion to this research is that using an insulation tank to decrease the heat loss might be a feasible and realistic option. The insulation tank has the same geometry as the reactor pressure vessel, in other words a cylinder in the middle with hemispheres at the top and the bottom. A practically feasible insulation tank is proposed and has the dimensions given in table (5.1).

Geometry dimensions	Name	Value
Deepest point of insulation tank	H	$18.4m$
Length of the insulation tank	L	$17.4m$
Outer diameter annulus	D_{an}	$3.6m$
Outer diameter reactor	D_{rpv}	$3.2m$
Depth in pool	$Depth$	$1m$
K value	K	2
Entrance cross-sectional area	A_{en}	$0.5m^2$

Table 5.1: Table with the final proposed geometry of the insulation tank.

With these dimensions the filling time of the insulation tank t_{fill} is $8.14[s]$. This result came out of the mechanical energy balance and is approximated using an implicit first order Taylor expansion. After the calculation of the filling time, an approximation of the temperature increase before the start of the cooling process is done.

The start of the cooling process is approximated as half the filling time. At that moment the tank is not full, but the water level passed half the tank and more than half of the tank therefore is already being cooled with flowing water. The temperature increase inside the reactor was calculated using two different methods. The first method was determining the density and specific heat capacity at two different temperature states. One temperature state being in the core and riser of the tank at the core outlet temperature of $396[^\circ C]$, according to the research of Krijger [5]. The second state was between $280 - 290[^\circ C]$, the core inlet temperature according to Krijger. The second method consisted of looking at the average density and specific heat capacity between the maximum and minimum temperatures. The pressure inside the reactor pressure vessel was assumed to stay constant. For the proposed dimensions of the insulation tank the temperature increases with $0.35[K]$ using both methods. Although this is a rough approximation, the temperature increase is considered reasonable and therefore follow-up study about the heat transfer is recommended.

5.2 Recommendations

This research continued on a recommendation Krijger [5] made for future research. While this research gives insight in the filling time and gives an approximation of the increase in heat, there are more steps to be taken to come to know the feasibility of such an insulation tank.

A necessary follow-up study after this research is doing heat transfer calculations with the insulation tank. It is important to calculate if the reactor remains inherently safe with an insulation tank filled with water. The steel layer might not be beneficial for the cooling process because this can be seen as extra isolation. On the other hand, many of the heat loss might come trough vaporizing the water, and via the entrance at the bottom cold water is keep being supplied.

Besides keeping the reactor inherently safe, it is important to investigate on the operational benefits of insulation and heat calculations during normal operations. The heat loss during normal operation must be investigated as well as the heat increase inside the reactor since there is less heat loss the environment during normal operation. If there is no safe geometry possible that ensures a significant lowering of heat loss an insulation tank does not have a function at all. When the heat loss to the environment is lower, a problem might occur that the reactor can become unstable. In the situation without the insulation tank, the water in the pool might act as a feedback system of the water inside the pool. When the water in the reactor heats up, the water is cooled more and therefore it may become more stable.

In this project is assumed that the water flows neatly into the tank, where in reality the water comes in slobbering and splashing. This is expected to have an effect on the filling time of the insulation tank. A study on the startup of this flow can be helpful to end up with a better approximation of reality.

Another study is whether the existing air pressure inside the insulation tank plays a significant role in the filling of the insulation tank and if in situation of SCRAM the power at the pump is able to fall away immediately as well as that a valve is opened where air could escape through. In this research these assumptions are made but they might not be valid assumptions.

References

[1] World Nuclear Association, Fukushima accident, October 2017, *<http://www.world-nuclear.org/information-library/safety-and-security/safety-of-plants/fukushima-accident.aspx>*. October 2017.

[2] I. N. Kessides, *The future of the nuclear industry reconsidered: Risks, uncertainties, and continued potential*, Energy Policy, 2012.

[3] D. Veling. *The Small-scale Large efficiency Inherent safe Modular Reactor*, November 2014.

[4] M. Rohde. *Safe and sustainable nuclear energy: the Thorium-based small, modular, supercritical water reactor.* VIDI proposal, 2012.

[5] D. Krijger. *Improving the performance of the SLIMR design*, November 2015.

[6] Giorgio Locatelli, Chris Bingham, Mauro Mancini. *Small modular reactors: A comprehensive overview of their economics and strategic aspects*, 2014.

[7] H. van den Akker, R. Mudde. *Fysische transportverschijnselen*, 2014.

[8] I. Pioro, S. Mokry. *Thermophysical Properties at Critical and Supercritical Conditions*, 2011. *<http://cdn.intechweb.org/pdfs/13204.pdf>*

[9] L.P.B.M. Janssen, M.M.C.G. Warmoeskerken. *Transport Phenomena Data Companion*, 2006.

[10] MATLAB Release 2015a, The MathWorks, Inc., Natick, Massachusetts, United States.

[11] The Mathworks, Inc., Evaluating Goodness of Fit, Natick, Massachusetts, United States. *<https://nl.mathworks.com/help/curvefit/evaluating-goodness-of-fit.html>*.

Appendix A

MatLab script with explicit solution

```
clear all
close all
clc

a=1;
g=9.81;
dt(1:a)=10^-4; [0.1:-0.01:0.02, 0.01:-10^-3:2*10^-3,
    10^-3:-10^-4:2*10^-4, 10^-4:-10^-5:2*10^-5, 10^-5:-10^-6:5*10^-6];
Dh=1;
L=17.4;
depth=1;
H=18.4;
K(1:a,1)=2;
mu25=0.89.*10.^-3;
rho25=997.05;
Aen=1;
Drpv=3.2;
Dan=4.2;
Dd=Dan-Drpv;
ha=13.2+Dan./2;
Dh=1;
Aan=pi./4.*(Dan.^2-Drpv^2);

v(1:a,1)=0;
h(1:a,1)=0;
t(1:a,1)=0;

for j=1:a
v(j,2)=sqrt(g.*H);
h(j,2)=v(j,2).*dt(1);
t(j,2)=dt(1);
for i=3:10^7

% if i <(1./dt)
%     P=0.1+0.9*(i.*dt).^(2);
% else
    P=1;
% end

    v(j,i)=v(j,i-1)+dt(j).*(g.*H.*P./h(j,i-1)-g-(1+(Aan.^2./Aen.^2).*K(
        j,1))/(2.*h(j,i-1)).*v(j,i-1).^2-(1/(-1.8.*log10(6.9.*mu25./(
        rho25.*v(j,i-1).*(Dh))))).^2./(2.*Dh).*v(j,i-1).^2);
    h(j,i)=h(j,i-1)+v(j,i).*dt(j);
```

```
        t(j,i)=t(j,i-1)+dt(j);
        if h(j,i)>=L
            tt(j)=t(j,i)
            break
        end
    end
end
```

Appendix B

MatLab script with implicit solution and decay heat calculations

```
clear all
close all
clc

a=1;
g=9.81;
dt(1:a)=10^-4; %[0.1:-0.01:0.02, 0.01:-10^-3:2*10^-3,
    10^-3:-10^-4:2*10^-4, 10^-4:-10^-5:2*10^-5, 10^-5:-10^-6:5*10^-6];
    %[10^-4:-10^-5:10^-5]; %10^-4
Dan(1:a)=3.6; %[5:-0.04:3.24]; %[5, 4.6, 4.2, 3.8, 3.4];
Drpv=3.2;
Dd(1:a)=Dan(1:a)-Drpv;
ha(1:a)=13.2+Dan(1:a)./2;
L(1:a)=16.4+Dd(1:a);
H(1:a)=18.4; %[17.4:0.1:21.4]; %[17.4, 18.4, 19.4, 20.4, 21.4];
K(1:a)=2; %[10, 7.5, 5, 2.5, 0]; %[10:-0.2:0];
Aen(1:a)=0.5; %[0.5:0.05:2.5]; %[0.5, 1, 1.5, 2, 2.5];
mu25=0.89.*10.^-3;
rho25=997.05;
Dh=1;
Aan(1:a)=pi./4.*(Dan(1:a).^2-Drpv^2);

v(1:a,1)=0;
h(1:a,1)=0;
t(1:a,1)=0;

for j=1:a
v(j,2)=sqrt(g.*H(j));
h(j,2)=v(j,2).*dt(1);
t(j,2)=dt(1);
for i=3:10^7

% if i <(1./dt)
%     P=0.1+0.9*(i.*dt)^(1./2);
% else
    P=1;
% end


A=[0, dt(j); dt(j).*(-g.*H(j).*P./(h(j,i-1).^2)+(1+(Aan(j).^2/Aen(j)
```

```
    .^2).*K(j)).*v(j,i-1).^2./(2*h(j,i-1).^2)), -dt(j).*(v(j,i-1).*(1+(
    Aan(j).^2/Aen(j).^2).*K(j))./h(j,i-1)+(1./(1.8.*log10(6.9.*mu25./(
    rho25.*v(j,i-1).*Dh)))).^2.*v(j,i-1)./Dh)];
B=[h(j,i-1); v(j,i-1)+dt(j).*(2.*g.*H(j).*P./h(j,i-1)-g+(1./(1.8.*log10
    (6.9.*mu25./(rho25.*v(j,i-1).*Dh)))).^2./(2.*Dh).*v(j,i-1).^2)];
I=[1 , 0; 0, 1];
X=mtimes(-(A-I)^-1,B);
h(j,i)=X(1,1);
v(j,i)=X(2,1);
t(j,i)=t(j,i-1)+dt(j);


    if h(j,i)>=L(j)
        tt(j)=t(j,i)
        break
    end
end
end

dt1=10^-4;
tt1=0:dt1:tt./2;
t1=tt1./(86400);
T0=5000; %running time
P0=350.*10^6; %power

WA=13.2.*pi.*1.23^2+4./3.*pi.*1.23^3; %Volume inside reactor
PS=0.2; %percentage of steel
RD=(pi.*0.47^2.*9)+4.25.*pi.*(1.37./2)^2; %Riser and core volume
ASH=WA.*((1-PS).*(RD./WA.*14000.*170+((WA-RD)./WA).*5000.*700)+PS
    .*460.*7700);
ASH2=WA.*((1-PS).*6000.*550+PS.*460.*7700);

P(1,1)=350*10^6;
J(1,1)=P(1,1).*dt1;
TI(1,1)=J(1,1)./ASH;
TI2(1,1)=J(1,1)./ASH2;

for k=2:length(tt1)
P(1,k)=6.48.*10.^-3.*(t1(1,k).^(-0.2)-(t1(1,k)+T0).^(-0.2)).*P0;
J(k)=J(1,k-1)+P(1,k).*dt1;
TI(k)=J(k)./ASH;
TI2(k)=J(k)./ASH2;
end
```